

On smoke suppression of clouds in Amazonia

Graham Feingold,¹ Hongli Jiang,² and Jerry Y. Harrington³

Received 30 August 2004; revised 24 November 2004; accepted 17 December 2004; published 19 January 2005.

[1] We use large eddy simulations of smoke-cloud interactions to demonstrate the relative importance of various factors responsible for cloud suppression in the biomass burning regions of Amazonia. The model includes unprecedented treatment of coupled smoke aerosol-cloud-radiative feedbacks in a 3-dimensional model that resolves scales of ~ 100 s m. It is shown that the vertical distribution of smoke aerosol in the convective boundary layer is crucial to determining whether cloudiness is reduced; Smoke aerosol emitted at the surface in a daytime convective boundary layer may reduce or increase cloudiness whereas smoke aerosol residing in the layer where clouds tend to form will reduce cloudiness. On the other hand, the reduction in surface latent and sensible heat fluxes associated with biomass burning is sufficient by itself to substantially reduce cloudiness. **Citation:** Feingold, G., H. Jiang, and J. Y. Harrington (2005), On smoke suppression of clouds in Amazonia, *Geophys. Res. Lett.*, 32, L02804, doi:10.1029/2004GL021369.

1. Introduction

[2] Hansen *et al.* [1997] proposed that absorbing aerosol may reduce cloudiness by modifying the heating rate profiles of the atmosphere. Absorbing aerosol heats and warms the atmosphere locally, modifies the atmospheric lapse rate of temperature and may suppress convection. This effect has been termed the “aerosol semi-direct effect”, and unlike the first and second aerosol indirect effects that respectively enhance cloud reflectance [Twomey, 1977] and increase cloud amount [Albrecht, 1989], the semi-direct effect is associated with a reduction in cloud fraction (CF).

[3] The semi-direct effect has been modeled at small scales ($\Delta x = 200$ m) using large eddy simulations (LES) by Ackerman *et al.* [2000] for conditions typical of Indian Ocean trade cumulus clouds. They simulated the diurnal cycle of clouds and imposed heating profiles associated with absorbing aerosol; heating was negligible near the surface, and focused in a layer 900 m thick where clouds tend to form. They showed decreases in cloudiness commensurate with the heating rates, thus illustrating Hansen *et al.*'s findings at the cloud scale. On the other hand, Norris [2001] examined a 42 year record of observed CF over the Indian Ocean and found a slight increase ($\sim 2\%$) in CF. They suggested that compensating factors such as increases

in sea surface temperature (SST) might partially explain this unexpected result.

[4] Johnson *et al.* [2004] studied the effects of absorbing aerosol on marine stratocumulus clouds using LES. They applied a number of different fixed aerosol profiles to show that the location of the absorbing aerosol is important; absorbing aerosol reduces cloud water when it resides in the boundary layer but, by reducing entrainment, increases cloud water when it lies above the cloud layer.

[5] Recent observations in Amazonia [Koren *et al.*, 2004] provide the first observational support for a reduction in CF due to smoke (absorbing) aerosol at a continental site. The authors demonstrated that CF decreases with increasing smoke optical depth τ_a . At $\tau_a = 0.6$ (at $0.5 \mu\text{m}$), cloudiness was reduced by 50% compared to the value at $\tau_a = 0.1$. They also suggested that in addition to stabilizing the atmosphere, smoke may affect cloudiness indirectly by reducing surface sensible and latent heat fluxes.

[6] The aforementioned studies provide incomplete and sometimes conflicting views of the effect of absorbing aerosol on clouds. Here we evaluate the relative importance of primary physical processes such as atmospheric stabilization, droplet heating, and surface flux modification using a new LES. The context is the convective, continental boundary layer, but we also consider the implications for aerosol effects on cloud development over oceans.

2. Model Description

[7] The LES is described by Feingold *et al.* [1996] with various upgrades as described below. The domain size is $6 \text{ km} \times 6 \text{ km} \times 4.5 \text{ km}$ with $\Delta x = \Delta y = 100 \text{ m}$ and $\Delta z = 50 \text{ m}$. The time step is 2 s. Simulations are based on a sounding on 26 September 2002 at 07:38 local time (11:38 UTC) from Fazenda, Brazil and are run for a little over 8 h (500 min). The study should not be viewed as a case study since the focus is on physical mechanisms, rather than comparisons with observations.

[8] Time series of surface latent and sensible fluxes derived from observations during the Smoke Aerosols, Clouds, Rainfall and Climate (SMOCC) experiment [Andreae *et al.*, 2004] are imposed at the surface; base conditions are taken from mean diurnal conditions averaged over the course of several months. The maximum sensible heat flux (190 W m^{-2}) and latent heat flux (340 W m^{-2}) occur at 13:00 local time. (A single simulation designed to reflect the effect of smoke on surface fluxes perturbs these fluxes, as described in section 3.) The model includes a size-resolved representation of aerosol and cloud drops; 14 size bins are used for aerosol and 12 bins suffice for drops because the clouds do not precipitate. Drop mass, drop number, and aerosol mass are accounted for in each drop size bin. The processes of activation, drop condensation/evaporation, coalescence, and sedimentation are simulated.

¹NOAA Environmental Technology Laboratory, Boulder, Colorado, USA.

²Cooperative Institute for Research in the Atmosphere/National Oceanic and Atmospheric Administration, Fort Collins, Colorado, USA.

³Department of Meteorology, Pennsylvania State University, University Park, Pennsylvania, USA.

Table 1. Description of Simulations and Mean Quantities Averaged Over 12–16 h Local Time^a

Name	Aerosol Heating	Fluxes	Smoke Location	LWP g m ⁻²	CF %	dθ/dz K km ⁻¹
S1	No	Observed	Surface	15.0	10.0	1.797
S2	Yes	Observed	Surface	16.9	9.9	0.157
S3	No	Observed	Aloft	20.4	10.7	1.908
S4	Yes	Observed	Aloft	3.6	5.0	3.363
S5	No	Reduced	Surface	1.6	2.7	6.897

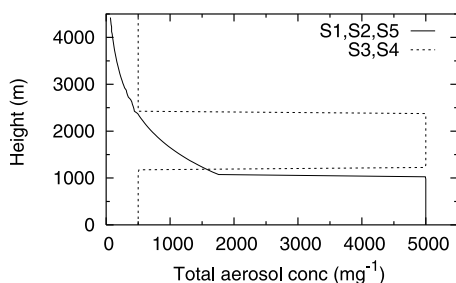
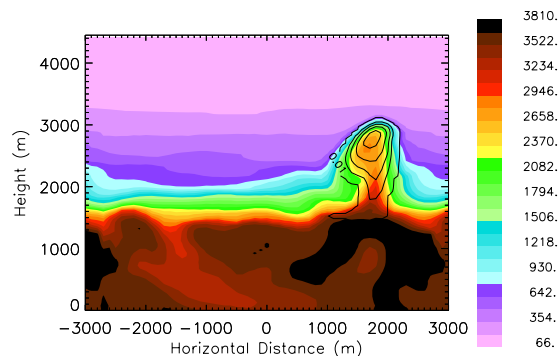
^aLWP is domain and time-averaged. dθ/dz is the lapse rate of potential temperature from 0–1500 m.

Tracking of aerosol within drops enables realistic simulation of cloud redistribution of aerosol.

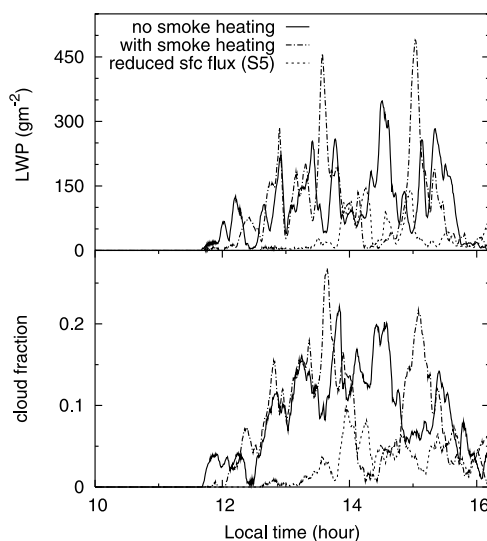
[9] The model's 8-band coupled radiation model [Harrington *et al.*, 2000] now includes the effects of a radiatively active aerosol. Smoke particle size distributions are initialized as lognormal distributions with $N_a = 5000 \text{ mg}^{-1}$ ($\sim 5000 \text{ cm}^{-3}$), $r_g = 0.1 \mu\text{m}$ and $\sigma_g = 1.5$. Particles are assumed to consist of a mix of soot and ammonium sulfate. Aerosol extinction and single scattering albedo ω_o are calculated based on this mix, and the ambient relative humidity. For the case to be presented, $\omega_o \sim 0.90$ at a wavelength of $0.47 \mu\text{m}$. Heating rates associated with smoke aerosol embedded inside droplets are calculated based on Conant *et al.* [2002]. The model thus includes the essential processes for simulating aerosol-cloud interactions and convective redistribution of aerosol within a coupled dynamical and radiative framework.

3. Results

[10] Five, three-dimensional simulations were performed as summarized in Table 1. All simulations consider $\tau_a = 0.6$ (dry) but differ (i) in whether they neglect or include the coupling of smoke heating with the dynamical model (e.g., S1 vs S2); (ii) in the vertical distribution of the smoke (e.g., S1 vs S3; Figure 1). (Examination of lidar profiles in Brazil during September 2002 indicates profiles that could be approximated by either of the profiles in Figure 1, with no clear preference.); (iii) in the magnitude of the surface fluxes (S1 vs. S5). Conditional instability in the initial sounding generates shallow convective clouds of $\sim 1000 \text{ m}$ – 1500 m in depth, with liquid water paths (LWP) of $\sim 200 \text{ g m}^{-2}$ (for individual cells) and CFs of ~ 0.05 – 0.25 . Figure 2 illustrates the aerosol concentration (the sum of interstitial and activated aerosol; color flooded contours) and the cloud liquid water content (LWC) (solid contours) at 14 h (local time) for simulation S1. The first comparison is between

**Figure 1.** Initial aerosol profiles for simulations S1–S5 as described in Table 1.**Figure 2.** Aerosol and smoke cross sections at 14 h illustrating typical clouds and vertical redistribution of smoke as initialized in S1. Color-flooded contours indicate aerosol concentration (unactivated + activated) in mg^{-1} and solid contours indicate LWC in g kg^{-1} (contour interval 0.5 g kg^{-1}).

simulations that investigate the effect of smoke heating when most of the aerosol is confined to the lowest 1200 m (S1 vs S2). Figure 3 and Table 1 respectively show that the domain and time averaged LWP and CF are similar. For both simulations clouds develop at around 11.7 h local time, determined primarily by the initial sounding. Smoke heating modifies the frequency and duration of cloudiness and there is even some indication of stronger convective events when smoke heating is included, as indicated by higher LWP at $t = 13.6 \text{ h}$ and $t = 15 \text{ h}$. Typical heating rates (Figure 4) associated with the smoke (S2) are $\sim 6 \text{ K day}^{-1}$ for the 11–12 h average, decreasing to $\sim 4 \text{ K day}^{-1}$ for the 14–15 h average as aerosol transport associated with boundary layer evolution spreads the heating over a deeper layer. These heating rates amount to solar absorption of $\sim 40 \text{ W m}^{-2}$ by the aerosol layer, which compares well with Yu *et al.* [2002] ($\sim 50 \text{ W m}^{-2}$). The radiatively active aerosol and cloud causes a reduction in the net solar fluxes at the surface of $\sim 100 \text{ W m}^{-2}$ which is comparable to the 40 – 100 W m^{-2} range of Kinne and Pueschel [2001]. The

**Figure 3.** Time series of liquid water path LWP and cloud fraction for simulations S1, S2, and S5.

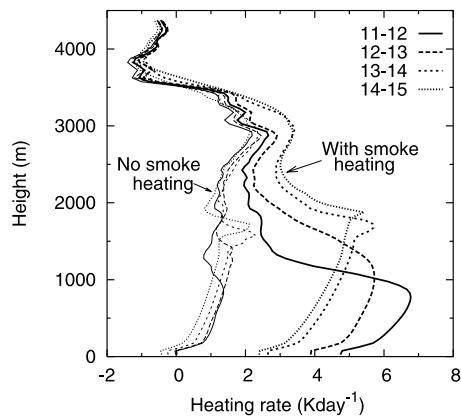


Figure 4. Radiative heating rate profiles for simulations S1 (no smoke heating, thin lines) and S2 (with smoke heating, thick lines). Line types refer to 1 h averages at local time.

effect of smoke heating is to destabilize the sub-cloud layer (Table 1). Without smoke heating (S1), the heating rates are $\sim 1 \text{ K day}^{-1}$.

[11] When comparing simulations S3 and S4 where aerosol is initially confined to a stable layer between $z = 1200 \text{ m}$ and 2400 m (Figure 1), smoke heating causes a distinct reduction in LWP and CF (Figure 5). (This heating rate profile is qualitatively similar to the one used by *Ackerman et al.* [2000].) The absorbing aerosol heats the atmosphere aloft and stabilizes the sub-cloud layer (Figure 6 and Table 1). Aerosol heating rate profiles that initially mimic the aerosol profile in Figure 1 are modified during the course of the simulation, as smoke is mixed and convected by the clouds (Figure 2). This initialization of the smoke slows the vertical mixing considerably so that heating rates tend to be higher than in case S2. Although the smoke heating spreads both above and below its initial location, the stabilization persists. Domain-averaged LWP decreases from 20.4 to 3.6 g m^{-2} and mean CF from $\sim 10\%$ to 5% .

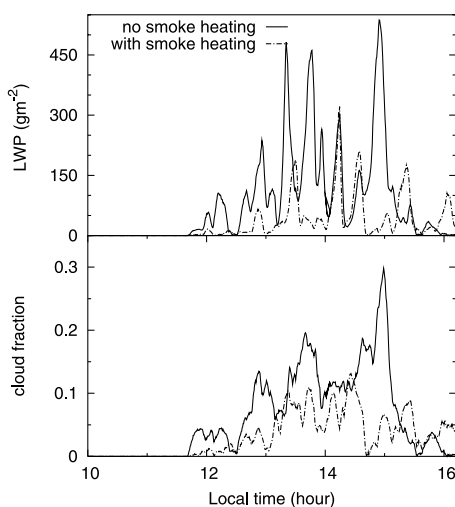


Figure 5. Time series of LWP and cloud fraction for simulations S3 (no smoke heating) and S4 (with smoke heating).

[12] The presence of aerosol reduces surface fluxes by reducing both the solar flux reaching the surface and evapotranspiration. Simulation S5 is a repeat of S1 but with one difference: the time-dependent surface fluxes are modified based on the numerical simulations of *Yu et al.* [2002] for similar τ_a and ω_o . The peak reductions in sensible and latent heat flux are -60 W m^{-2} and -70 W m^{-2} , respectively. An analysis of the Aerosol Robotic Network and surface flux data for arbitrary thresholds of clean and polluted conditions supports the sign of these perturbations. Figure 3 and Table 1 show a strong reduction in cloudiness due to the reduced surface fluxes indicating that this factor alone is sufficient to explain the observed reduction in cloudiness in biomass burning regions of Brazil. In this simulation, the sub-cloud layer is significantly more stable than in all of the others (Table 1).

4. Discussion

4.1. Vertical Distribution of Smoke

[13] The results reinforce the fact that the location of the aerosol and associated heating is crucial to determining whether cloud cover will change, and this factor may affect the sign of the change. When smoke is initially confined to the sub-cloud layer, cloud LWP and CF may even increase (Table 1; S1 vs S2). We have analyzed numerous two-dimensional simulations that indicate this result is robust. The smoke aerosol mixes through the sub-cloud layer and distributes its heating fairly uniformly so that stabilization does not occur. Instead, the added heat associated with the smoke may destabilize the sub-cloud layer (Table 1) and increase convection.

[14] There is a clear reduction in cloud amount when the smoke aerosol is initially confined to the layer in which clouds tend to form (Table 1; S3 vs S4), or when surface fluxes are reduced (S1 vs S5). The reduction in CF by more than half is in close agreement with *Koren et al.* [2004] for similar τ_a , and consistent with *Ackerman et al.*'s [2000] 40% reduction in CF for $\tau_a = 0.4$ (and similar ω_o). In the case of simulation S4, the primary reason for the reduction in CF and LWP is the increased stabilization of the cloud layer and not the heating associated with smoke embedded

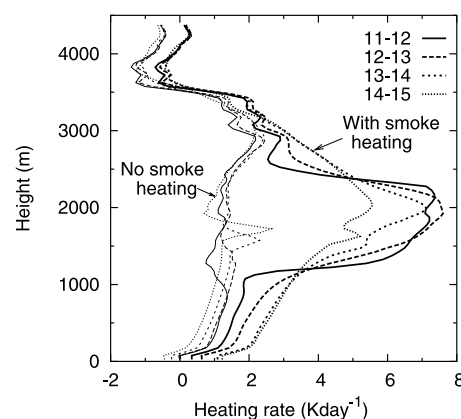


Figure 6. Radiative heating rate profiles for simulations S3 (no smoke heating, thin lines) and S4 (with smoke heating, thick lines). Line types refer to 1 h averages at local time.

inside the drops (as studied by *Conant et al.* [2002]), which we found incurs only minor changes in cloud evolution.

4.2. Surface Flux Modification

[15] The simulations have not coupled the response of surface fluxes to smoke aerosol and clouds, but have imposed surface fluxes based on observations in Amazonia. This helps to isolate the surface forcing from an already tightly coupled system. A full coupling with a surface model would allow surface fluxes and temperatures to respond more naturally to the evolving aerosol and cloud fields but this is not expected to produce qualitative changes in results. For the simulation presented here, a reduction in surface fluxes associated with smoke has been demonstrated to be sufficient to substantially reduce clouds without invoking arguments based on aerosol profiles generating a more stable boundary layer. This is important over land but not over the ocean where surface fluxes are much less variable. As previously noted, the multi-decadal study of clouds over the Indian Ocean by *Norris* [2001] indicates a small increase in CF with increasing aerosol. If the stabilizing effect of lofted aerosol were important one might have expected a steady decrease in CF. The fact that this is not the case could be rooted in three factors: (i) During the Indian Ocean Experiment (INDOEX) elevated aerosol layers residing above the cloud layer were observed about 2/3 of the time [*Ramanathan et al.*, 2001]. The resultant strengthening of the capping inversion could help sustain a shallower and moister cloud layer [*Johnson et al.*, 2004]; (ii) Increased cloud lifetime due to a suppression of precipitation, although this appears to be unimportant in the region studied by *Norris* [2001]; (iii) An increase in SST over the four decade period might partially explain the higher CF [*Norris*, 2001]. However, the relationship between SST and CF is ambiguous since an increase in SST may occur in concert with other compounding meteorological factors such as changes in the humidity profile.

5. Summary

[16] This paper has demonstrated that the reduction in surface fluxes associated with smoke [*Yu et al.*, 2002] is the simplest explanation for the observed reduction in cloudiness in continental, convective boundary layers that produce clouds of ~ 1 km in depth [*Koren et al.*, 2004]. Cloud fraction may also be significantly reduced if elevated smoke layers stabilize the cloud layer. However, smoke resident in the well-mixed boundary layer does not suppress cloud formation and may even enhance it. The results may also explain the discrepancy between the modeled reduction in cloudiness over the Indian Ocean [*Ackerman et al.*, 2000] and the observed increase in cloudiness [*Norris*, 2001]; The observed preponderance of aerosol above the cloud layer during INDOEX would tend to reduce entrainment and help maintain a moister cloud layer and higher cloud fraction [*Johnson et al.*, 2004]. Natural variability in the vertical

distribution of absorbing aerosol (or a higher concentration of surface aerosol) would also be consistent with no change (or an increase) in cloud fraction with increasing aerosol.

[17] We note that these results have been derived from a single sounding and a single smoke aerosol size distribution. The effects of smoke aerosol on both heating rates and reduction in surface fluxes will be case specific; in this study, significant reductions in cloud fraction are achieved with smoke optical depths (visible) of about 0.6, in broad agreement with observational and modeling studies. Modifications to cloudiness will in general be a function of cloud type and commensurate with the smoke optical properties, the location of the aerosol, and the extent of reduction in surface fluxes.

[18] **Acknowledgments.** We thank J. V. Martins, I. Koren, L. Remer, and Y. Kaufman for useful discussions, the reviewers for useful comments, and the SMOCC science team for sounding and surface flux data. This research was supported by a NASA IDS grant, NOAA's Climate and Global Change Program, and an NSF grant ATM-0234211 (JYH).

References

- Ackerman, A. S., et al. (2000), Reduction of tropical cloudiness by soot, *Science*, *288*, 1042–1047.
- Albrecht, B. A. (1989), Aerosols, cloud microphysics, and fractional cloudiness, *Science*, *245*, 1227–1230.
- Andreae, M. O., et al. (2004), Smoking rain clouds over the Amazon, *Science*, *303*, 1337–1342.
- Conant, W. C., A. Nenes, and J. H. Seinfeld (2002), Black carbon radiative heating effects on cloud microphysics and implications for the aerosol indirect effect: 1. Extended Köhler theory, *J. Geophys. Res.*, *107*(D21), 4604, doi:10.1029/2002JD002094.
- Feingold, G., S. M. Kreidenweis, B. Stevens, and W. R. Cotton (1996), Numerical simulation of stratocumulus processing of cloud condensation nuclei through collision-coalescence, *J. Geophys. Res.*, *101*, 21,391–21,402.
- Hansen, J., M. Sato, and R. Ruedy (1997), Radiative forcing and climate response, *J. Geophys. Res.*, *102*, 6831–6864.
- Harrington, J. Y., G. Feingold, and W. R. Cotton (2000), Radiative impacts on the growth of a population of drops within simulated summertime Arctic stratus, *J. Atmos. Sci.*, *57*, 766–785.
- Johnson, B. T., K. P. Shine, and P. M. Forster (2004), The semi-direct aerosol effect: Impact of absorbing aerosols on marine stratocumulus, *Q. J. R. Meteorol. Soc.*, *30*, 1407–1422.
- Kinne, S., and R. Pueschel (2001), Aerosol radiative forcing for Asian continental outflow, *Atmos. Environ.*, *35*, 5019–5028.
- Koren, I., Y. J. Kaufman, L. A. Remer, and J. V. Martins (2004), Measurement of the effect of Amazon smoke on inhibition of cloud formation, *Science*, *303*, 1342–1345.
- Norris, J. R. (2001), Has northern Indian Ocean cloud cover changed due to increasing anthropogenic aerosol?, *Geophys. Res. Lett.*, *28*, 3271–3274.
- Ramanathan, V., et al. (2001), Indian Ocean Experiment: An integrated analysis of the climate forcing and effects of the great Indo-Asian haze, *J. Geophys. Res.*, *106*, 28,371–28,398.
- Twomey, S. (1977), The influence of pollution on the short wave albedo of clouds, *J. Atmos. Sci.*, *34*, 1149–1152.
- Yu, H., S. C. Liu, and R. E. Dickinson (2002), Radiative effects of aerosols on the evolution of the atmospheric boundary layer, *J. Geophys. Res.*, *107*(D12), 4142, doi:10.1029/2001JD000754.

G. Feingold, NOAA Environmental Technology Laboratory, 325 Broadway, Boulder, CO 80305, USA (graham.feingold@noaa.gov)
 J. Y. Harrington, Department of Meteorology, Pennsylvania State University, University Park, PA 16802, USA. (harring@mail.meteo.psu.edu)
 H. Jiang, CIRA/NOAA, Fort Collins, CO 80531, USA. (jiang@atmos.colostate.edu)